AIChE

Properly Calculate Vessel and Piping Wall Temperatures During Depressuring and Relief

Georges A. Melhem and David Gaydos
ioMosaic Corporation, 93 Stiles Road, Salem, NH 03079; Gaydos.d.nh@iomosaic.com (for correspondence)

Published online 17 June 2014 in Wiley Online Library (wileyonlinelibrary.com). DOI 10.1002/prs.11689

Determining if and when a vessel and/or piping component is going to fail under fire exposure and/or from cold temperature embrittlement is an important factor in consequence analysis and risk assessment. This article describes detailed methods for establishing the conditions for vessel/piping failure and whether the material of construction for vessels and piping is properly selected for fire exposure and/or cold depressuring/relief.

Several case studies are used to illustrate important concepts dealing with how wall temperatures should be calculated for single and multiphase systems in order to establish if a vessel and/or a piping component is going to fail. © 2014 American Institute of Chemical Engineers Process Saf Prog 34: 64–71, 2015

Keywords: fire exposure; vessel failure; relief systems; depressuring systems; embrittlement; flame jets; wall temperatures; hoop stress; pool fires

INTRODUCTION

Loss of containment scenarios caused by catastrophic vessel and piping failures can lead to severe consequences including fire, explosion, blast wave damage, or a toxic cloud moving across the property and into the surroundings. The proper quantification and understanding of scenario frequencies, actual vessel and piping failure potential, and any associated consequences can provide for better risk management and allocation of resources for risk reduction.

Vessels and piping components can fail because of excessive deviations in internal or external pressure and/or wall temperatures. Other causes of vessel and piping component failures not considered in this article include corrosion under insulation, manufacturing defects, external impact, etc.

A classic scenario that is almost always considered in risk assessments is the exposure of a process/storage vessel and piping components to a pool fire or flame jet. The heat input from the fire causes the pressure and temperature of the contents as well as the temperature of the metal walls to increase. As the wall temperature increases, the metal strength decreases, and if the internal pressure is high enough, loss of containment will occur. If the contents are flammable, and depending on the size of the vessel contents, a spectacular fireball and/or vapor cloud explosion can follow. There is a substantial difference in the likelihood of vessel failure, depending on whether the exposure is caused by a pool fire or a flame jet and whether the dry wall is exposed to fire.

Flame jet impingement causes high intensity localized heating. Because jets are efficient mixers, the wall impinged area can receive a time average fire flux as high as 350 kW/m^2. The intense heating of the jet fire causes the exposed metal to heat up, which reduces its tensile strength. If the heating continues, the wall temperature may eventually reach the vessel's ultimate tensile strength (UTS) and rupture may take place. Failures caused by flame jet impingements on the vapor space (no liquid) typically occur within a few minutes, for example, on the order of 5 min.

Heating rates caused by total pool fire engulfment, partial engulfment, or thermal radiation (pool fire from a distance) will depend on the fuel type, burning rate, pool diameter size, flame height, flametilt, flame drag, atmospheric transmissivity, and geometric view factor. A typical average fire flux associated with a C_7 hydrocarbon pool fire is on the order of 60 kW/m^2. Lighter hydrocarbon pool fires, especially liquefied natural gas (LNG) fires, can produce more intense heating with peak fire flux values well in excess of 250 kW/m^2. Most of the heat absorbed into the vessel contents is absorbed by the liquid. (Wetted surface area is typically used for that reason.) This is because of the poor heat transfer between the vapor contents and the vapor walls from natural convection. Typical failures will occur at the vapor/liquid interface because of increased thermal stress due to the difference in temperature between the vapor space hot metal and liquid space cooler metal.

We should note that vessels containing reactive materials require special attention since fire-induced runaway reactions will occur at exponential rates, leading to the generation of more internal heat and/or gases and vapors.

The failure potential can be mitigated using fixed water sprays, pressure relief devices, and/or emergency depressuring valves. Passive mitigation in the form of fire proof insulation can also be used if careful consideration is given to corrosion under insulation that may occur. Additional mitigation options including reaction inhibiters, quench fluids, etc. are also considered for reactive systems. Rapid fire detection and isolation of the fuel source can also reduce the likelihood of failure. Other means exist for mitigation including sloping, segregation of flammable inventories, reduction of flammable inventories, etc. Note that pressure relief valves (PRV) cannot protect a vessel from extended fire exposure if the unwetted wall is exposed to the fire. The PRV will continue to open and reseat and ultimately the dry metal wall will weaken enough to fail at the reseat pressure of the PRV. Rupture disks and/or automated depressuring valves, when properly sized, can reduce the pressure fast enough to outpace the decline in metal strength caused by increasing temperatures. Depressuring systems and fire-proof insulation may be the only credible means for mitigating flame jet impingement. Water sprays may not be effective in mitigating high pressure flame jets. At the point of flame jet impact, the force of the jet can result in a dry spot where intense heating would be localized. Fixed water sprays can be an effective mitigation measure for pool fires.

Rapid depressurization can cause cryogenic temperatures in pressure vessels and also in the piping downstream of the depressuring valves due to expansion cooling and condensation of light ends. This is especially a problem in gas processing facilities and facilities with high pressure systems.

The primary objective of this article is to describe detailed methodologies that can be used to determine if and when a vessel or piping components will fail under fire exposure, with and without a chemical reaction. An important aspect of the modeling methodologies described in the article is the ability to assess the impact of mitigation measures on the failure potential.

CALCULATION OF FIRE FLUX

In order to determine if a vessel is going to fail under fire exposure, we need to determine how much heat is absorbed by the external vessel surface (metal or insulation), and how much of that heat is absorbed by the vessel contents. Popular methods for establishing heating rates into vessels include the American Petroleum Institute (API) standard 521 [1] and National Fire Protection Association (NFPA) Flammable and Combustible Liquids Code NFPA-30 [2] (see Figure 1). These correlations are based on large scale test data with heavy hydrocarbons and on a measurement of how much heat is gained by the vessel contents and not the vessel walls.

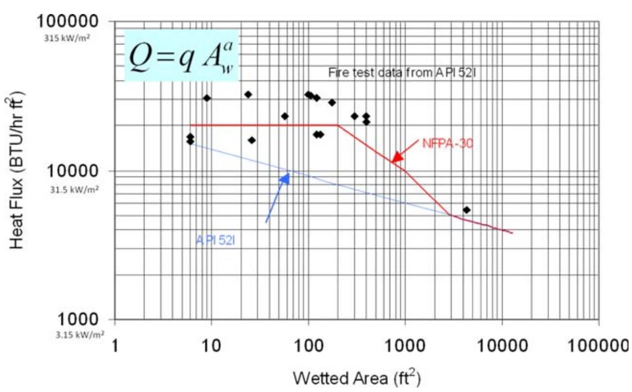

Figure 1. NFPA-30 and API-521 fire flux correlations. [Color figure can be viewed in the online issue, which is available at **wileyonlinelibrary.com**.]

The total heating rate absorbed by the vessel contents is correlated with the wetted surface area according to the following simple empirical expression:

$$Q = qFA_w^a \tag{1}$$

where Q is the total heating rate absorbed by the liquid in Watts, F is a mitigation factor that is used to allow reduction of the heating rate because of water sprays, firefighting, and/or insulation, and A_w is the wetted surface area in m^2, that is, the area contacted by liquid. The constant q represents the heat flux absorbed by the liquid, corrected for the presence of adequate drainage. Note that q includes a unit conversion factor associated with the fact that the wetted surface area is raised to a power less than 1. Equation 1 correlates the heat absorbed by the vessel contents to the wetted surface area raised to a power of 0.82 in the case of API-521. Note that the NFPA-30 and API-521 correlations differ for wetted surface areas that are less than 2,800 ft^2, with NFPA-521 yields a higher heating rate.

The NFPA-30 and API-521 correlations are primarily used to establish the relief requirements and should not be used to establish vessel wall temperatures or to assess vessel integrity. The total heating rate obtained from these correlations is divided by the liquid latent heat of vaporization to establish the vaporization rate (vapor generation rate) that needs to be vented at a permissible vessel overpressure, typically 21% of the maximum allowable working pressure (MAWP). The heating rates calculated by these correlations are underpredicted for light hydrocarbons and overpredicted for heavy hydrocarbons, as illustrated in Table 1. The fuel-specific factor (FF) developed in this article is established based on literature reported data of pool fires, detailed modeling estimates, and data provided by API-521 suggesting that approximately 75% of the fire flux is typically absorbed by the vessel liquid contents [3].

The FF developed in this article as shown in Table 1 can also be calculated using the following equation:

$$FF = 2.25 - 0.006T_{NBP} \tag{2}$$

where T_{NBP} is the normal boiling point in °F, and is less than 345°F. More recently, Zamejc [4] recommended that, for confined pool fires, the exponent of the simple API-521 Eq. 1

Table 1. Recommended fuel-specific factors for use with NFPA-30/API-521 simple heating rate correlations (Eq. 1).

Fuel	Carbon Number	Normal Boiling Point (°F)	Estimated Flame Emissive Power (kW/m^2)	Fuel Factor. Multiply the calculated heating rate obtained from Eq. 1 by this factor
Methane	C_1	−258.68	198	3.8
Ethane	C_2	−127.48	157	3.0
Propane	C_3	−43.67	131	2.5
Butane	C_4	31.10	107	2.0
Pentane	C_5	96.92	87	1.7
Hexane	C_6	155.71	68	1.3
Heptane	C_7	209.17	52	1.0
Octane	C_8	258.22	36	0.7
Nonane	C_9	303.48	22	0.5
Decane	C_{10}	345.48	20	0.5

Table 2. Recommended parameter values for Eq. 3 for flame jets by API-521 [1] where other data or information are unavailable.

		Flame Jet			
Parameter	Description	Surface Average Heat Flux		Local Peak Heat Flux	
Leak rates		>2 kg/s (Large Jet)	≤2 kg/s (Small Jet)	>2 kg/s (Large Jet)	≤2 kg/s (Small Jet)
ε_f	Flame emissivity	0.33	NA	0.87	0.75
ε_w	Wall emissivity	0.75	NA	0.75	0.75
α_w	Wall absorptivity	0.75	NA	0.75	0.75
h	Convective heat transfer coefficient between equipment and surrounding air	40 W/m^2 K	NA	100 W/m^2 K	90 W/m^2 K
T_g	Temperature of combustion gases flowing over the surface	1,173 K (900°C)	NA	1,473 K (1,200°C)	1,373 K (1,100°C)
T_f	Fire temperature	1,373 K (1,100°C)	NA	1,473 K (1,200°C)	1,373 K (1,100°C)
q_f	Fire heat flux	100 kW/m^2	NA	350 kW/m^2	250 kW/m^2
q_w	Absorbed heat flux	85 kW/m2	NA	290 kW/m^2	210 kW/m^2

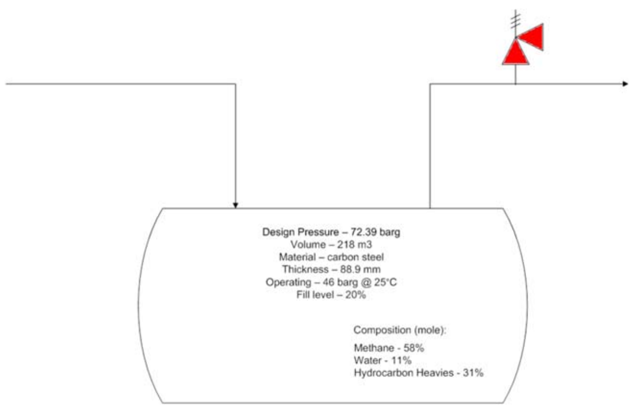

Figure 2. Case study A. [Color figure can be viewed in the online issue, which is available at **wileyonlinelibrary.com**.]

can be raised from 0.82 to 1. He considered a pool fire to be confined when the equipment under fire is partially confined by adjacent embankments or walls equal or greater than the equipment height.

A much better procedure for estimating the heating rate into the walls and the vessel contents is the more fundamental equation recently included in the latest revision of API-521 [1]:

$$q_w = \alpha_w \varepsilon_f \sigma T_f^4 + h\left(T_{f,g} - T_{w,t}\right) - \varepsilon_w \sigma T_{w,t}^4 \qquad (3)$$

The first term in Eq. 3 is the flame radiative heat flux into the external wall or insulation surface. The second term is the hot combustion gases convective heat flux into the external wall or insulation surface. The third term is the heat flux that is reradiated by the external wall or insulation surface. Note that temperature in this equation must be absolute, either in Kelvin or Rankin.

If SI units are used, q_w is the net heat flux reaching the wall or insulation surface in W/m^2/K, α_w is the external wall surface or insulation absorptivity, ε_f is the flame surface emissivity, σ is the Stefan–Boltzman constant = 5.67 × 10^{-8} W/m^2/K^4, T_f is the flame surface temperature in K, h is the combustion gases convective heat transfer coefficient in W/m^2/K, $T_{f,g}$ is the combustion gases temperature in K, $T_{w,t}$ is the time dependent wall surface temperature, and ε_w is the external wall or insulation surface emissivity.

Recommended values are provided by API-521 [1] for a typical unconfined heptane pool fire engulfing an uninsulated carbon steel vessel for a surface average heat flux ($\alpha_w = 0.75$, $\varepsilon_f = 0.75$, $T_f = 750$°C (1,023 K), $h = 20$ W/m^2/K, $T_{f,g} = 600$°C (873 K), and $\varepsilon_w = 0.75$) and local peak heat flux parameters ($\alpha_w = 0.75$, $\varepsilon_f = 0.75$, $T_f = 1{,}050$°C (1,323 K), $h = 20$ W/m^2/K, $T_{f,g} = 1{,}050$°C (1,323 K), and $\varepsilon_w = 0.75$). These recommended values are consistent with a fire flux of 60 kW/m^2 and 150 kW/m^2 for surface-averaged and local peak values and wall absorbed values of 45 kW/m^2 and 120 kW/m^2, respectively. Recommended values for jet fires are also provided by API-521 [1] (as shown in Table 2) where actual test data are not readily available for establishing the flame characteristics.

Melhem [5] showed that the simple API-521 equation (Eq. 1) can be recovered from Eq. 3 when the dynamics are properly modeled. Equation 3 can be used to develop both the relief requirements and to assess the failure potential as well as the use of a variety of mitigation options. Melhem [5] also independently demonstrated that Eq. 3, when used with SuperChems Expert™ vessel and wall dynamics, can accurately reproduce measured large scale BAM (Bundesanstalt für Materialforschung und - prüfung) [6] fire exposure test data including wall temperatures and vessel failure pressure.

We present next three case studies that illustrate the use of Eq. 3 to assess vessel failure potential under fire exposure.

CASE STUDY A

We consider the case of a process vessel exposed to a 2-hour simple API-521 fire (Eq. 1). The PRV is sized such the maximum pressure in the vessel that is reached during the fire is less or equal to 1.21 × MAWP. This example is illustrated in Figure 2.

The relief requirement is established using Eq. 3 and the parameters provided by API-521 [1] listed in Table 3 for surface average heat flux. The surface average heat flux of 45 kW/m^2 applied to wetted surface area is used to calculate the total heat input into the process fluid from a pool fire. We can show using dynamics that the pressure in the vessel based on the API-521 heating rate absorbed by vessel contents will stay below 1.21 × MAWP. The pressure time history is illustrated in Figure 3. While this is currently an

Table 3. Recommended parameter values for Eq. 3 for open pool fire by API-521 [1] where other data or information are unavailable.

		Pool Fire	
Parameter	Description	Surface Average Heat Flux	Local Peak Heat Flux
ε_f	Flame emissivity	0.75	0.75
ε_w	Equipment emissivity	0.75	0.75
α_w	Equipment absorptivity	0.75	0.75
h	Convective heat transfer coefficient between equipment and surrounding air	20 W/m^2 K	20 W/m^2 K
T_g	Temperature of combustion gases flowing over the surface	873 K (600°C)	1,323 K (1,050°C)
T_f	Fire temperature	1,023 K (750°C)	1,323 K (1,050°C)
q_f	Fire heat flux	60 kW/m^2	150 kW/m^2
q_w	Absorbed heat flux	45 kW/m2	120 kW/m^2

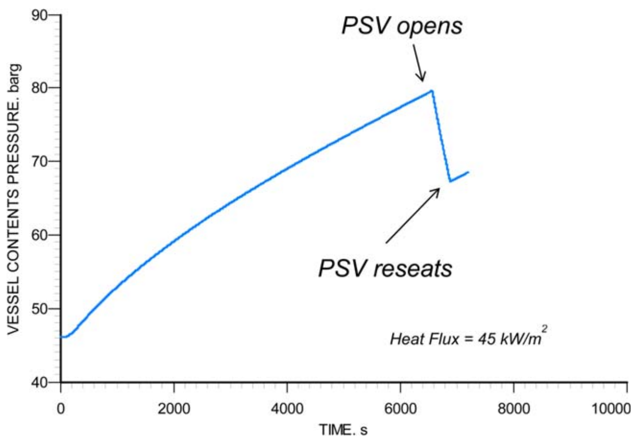

Figure 3. Case study A—Vessel pressure history. [Color figure can be viewed in the online issue, which is available at **wileyonlinelibrary.com**.]

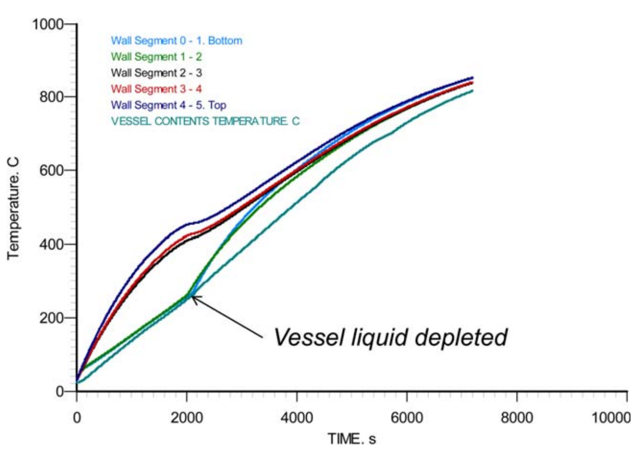

Figure 4. Predicted wall segments temperatures using SuperChems Expert^{TM} and Eq. 3. [Color figure can be viewed in the online issue, which is available at **wileyonlinelibrary.com**.]

acceptable practice, it is well known that a PRV cannot protect a vessel from failure for extended fire duration. A properly sized PRV has to reseat and, if the fire continues, the vessel will ultimately fail at the reseat pressure of the PRV.

To illustrate this case, we divide the vessel into five segments and use the dynamics provided in SuperChems Expert^{TM} to estimate the relief and wall temperature dynamics. The heat flux for this case is determined using Eq. 3 and the parameters provided by API-521 [1] listed in Table 3 for local peak heat flux. The local peak heat flux of 120 kW/m^2 is used in the simulation since the intent is to calculate the localized maximum wall temperature which affects metal strength. The temperature profiles for all five vessel metal segments are shown in Figure 4. As expected, the walls in contact with the vapor space become hotter than the walls in contact with the liquid space. We note that the liquid level is ultimately depleted (vaporized), and once the liquid level is depleted, the metal segments that become dry are heated more quickly.

One needs to also consider the impact of the onset of two-phase flow from a relief device and/or a depressuring valve when they are actuated. The heat stored in the vapor walls can ultimately be recovered by the vessel contents during two-phase swell and/or flow since the vapor walls will get coated with a two-phase mixture. Since we know the metal wall segment temperatures and we also know the pressure history as a function of time, we can estimate the internal hoop stress the metal segments are exposed to and decide if the metal is likely to fail. We consider two-third of the UTS to be the failure boundary instead of 100%. A safety factor is normally recommended to account for uncertainties associated with metal properties, defects, and calculation methods.

The failure stress of each metal segment is shown in Figure 5 as is the internal hoop stress. The failure stress (UTS) reduces rapidly after 2,000–3,000 s when the wall temperature reaches 450–500°C. This vessel is predicted to fail in approximately 1 h. If there is sufficient fuel inventory to sustain a fire for an hour, the PRV is not going to protect the vessel from failure.

A properly sized depressuring valve can reduce the pressure (stress) in the vessel faster than the reduction of tensile strength caused by fire heating. In the absence of detailed modeling tools that consider the wall temperature dynamics, API-521 [1] recommends reducing the internal pressure to 50% of the design pressure within 15 min of the fire

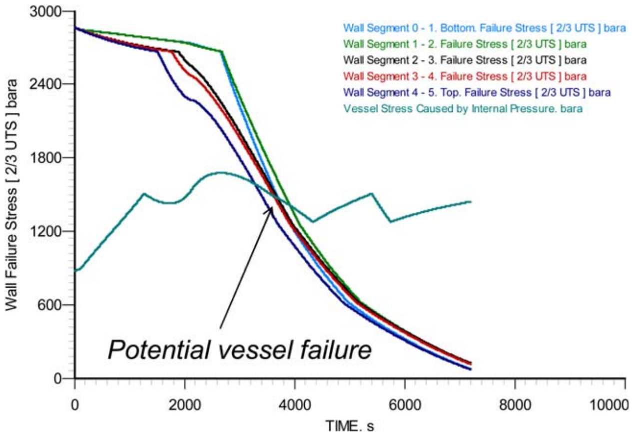

Figure 5. Case study A—Predicted failure pressure. [Color figure can be viewed in the online issue, which is available at **wileyonlinelibrary.com**.]

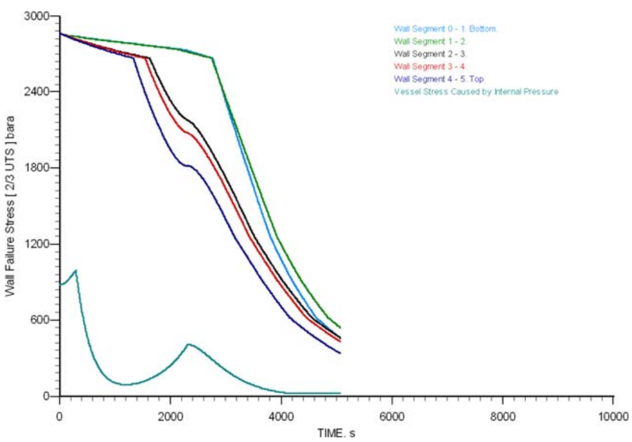

Figure 6. Case study A—Predicted failure stress with an emergency depressuring valve. [Color figure can be viewed in the online issue, which is available at **wileyonlinelibrary.com**.]

scenario. Note that this criterion is for 1-inch thick steel only. Stainless steel vessels may sustain higher pressures than specified and vessels with wall thickness that is less than 1 in. may fail at lower pressures than specified.

Reduction in pressure to 100 psig is suggested in API-521 [1] for vessel leaks. Fifteen minutes is recommended in the current version of API-521 [1]. The criteria recommended by API-521 are not effective for flame jet impingement. A depressuring time of 5 min or less is more appropriate and needs to be confirmed using dynamics.

It can be demonstrated that, in this case, equipping our process vessel with a properly sized depressuring valve to reduce the pressure to 100 psig in 15 min will protect the vessel from failure during an extended fire exposure as shown in Figure 6. Other mitigation measures that can be explored are the use of fire proof insulation, fixed water sprays, etc.

Although not illustrated here, modeling of the system dynamics can be very useful and can provide insight into the proper selection of insulation thickness, actuation time of the depressuring system, water spray density requirements, etc. More importantly, dynamics are very useful to study the sensitivity of the final design to key mitigation parameters or system characteristics.

CASE STUDY B—DEPRESSURING SYSTEMS

The use of depressuring systems is common in the oil and gas industries. For these systems, we have to consider the impact of cold temperatures as well as high temperatures. Cold temperatures reached in a vessel that is being depressured or downstream of the depressuring valve (especially if dew point is reached) can reach or exceed the minimum allowable design metal temperature. Extremely cold temperatures can be reached for high pressure systems and can be well below the embrittlement temperature of carbon steel. Carbon steel is typically used in services with temperatures above $-20°F$. At temperatures below $-20°F$, normal carbon steel loses ductility and strength, and the metal becomes brittle and can be susceptible to brittle fracture. Brittle fracture requires three contributing factors to be present: (a) a susceptible steel at cold temperature, (b) a crack or notch typically found in weld defects, (c) and an applied stress that is large enough to cause failure (7 ksi or more for carbon steel).

Condensing vapor/two-phase flow downstream of the depressuring valve can lead to more liquid accumulation in downstream vessels and enhanced heat transfer between the vessel/piping components walls and the vessel/pipe fluid contents. For hydrocarbon systems containing water, hydrate formation also becomes a concern. High superficial velocities can be reached during depressuring for high pressure systems, which can cause two-phase flow and enhanced heat transfer between the vessel fluid contents and walls.

Heat transfer between the vapor/gas in the vapor space and the walls of a vessel that is being depressured is typically very poor and is dominated by natural convection. This is only true for noncondensing systems, that is, where the dew point is not reached during depressuring. If condensation occurs during depressuring, the heat transfer becomes more pronounced and cold liquids can collect in the bottom of vessels. This condensation can cause embrittlement failure of the metal wall sections exposed to the cold liquid.

We consider one test from the 1992 large scale depressuring test series conducted by Haque *et al.* [7] to illustrate the poor heat transfer characteristics of noncondensing systems using nitrogen. The dataset contained sufficient details for the vessel and starting conditions. A vertical cylindrical vessel ($L = 1.524$ m, Flat Head, ID = 0.273 m, 25-mm wall thickness) containing nitrogen was depressured through a 6.35-mm equivalent flow orifice. The initial pressure and temperature conditions were reported to be 150 bar and 20°C. Mass release rates and the actual flow orifice details were not reported.

This test was reproduced using SuperChems Expert™. The heat transfer coefficients used in SuperChems Expert™ are based on literature correlations without any adjustable parameters. The user can, however, define specific fixed heat transfer coefficients for both the liquid and vapor space. The calculated pressure profile is shown in Figure 7 and is an excellent agreement with the reported measured data.

One should note that, while it is always possible to obtain a reasonable representation of the pressure profile for depressuring systems using a pseudovolume approach, temperature predictions require very detailed analysis, especially where the depressuring system has several interconnected vessels with different surface to volume ratios and metal thicknesses. Special attention should be paid to interconnecting piping segments and vessels with thin walls that are exposed to fire.

The calculated temperatures for the gas and the walls are also in very good agreement with the measured data. This is

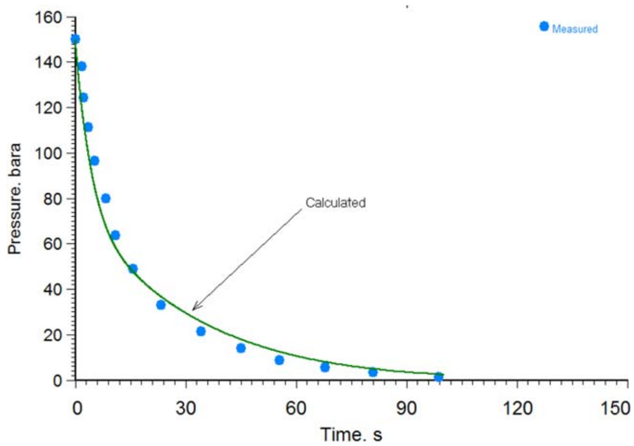

Figure 7. Case study B—Calculated pressure profile. [Color figure can be viewed in the online issue, which is available at **wileyonlinelibrary.com**.]

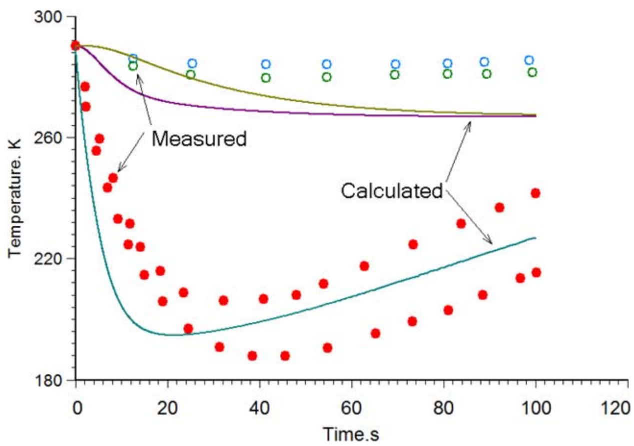

Figure 8. Case study B—Fluid and wall temperature predictions. [Color figure can be viewed in the online issue, which is available at **wileyonlinelibrary.com**.]

shown in Figure 8. The solid and hollow circles represent actual measurements at different locations in the vessel. Natural convection heat transfer coefficients for gases and vapors are usually on the order of 100 W/m^2/K, while heat transfer coefficients for boiling liquids under fire exposure and for condensing vapors during depressuring are substantially higher. API-521 [1] suggests that heat transfer coefficients for boiling multicomponent hydrocarbon liquids under fire exposure range from 1,000 to 3,000 W/m^2/K. The predictions calculated in this article for this large scale dataset indicate that the existing literature published correlations for heat transfer used in SuperChems Expert^{TM} have good predictive capabilities.

CASE STUDY C—PIPE FLOW

As indicated earlier, cold embrittlement temperatures can also be exhibited downstream of the depressuring valve, especially for high pressure systems. This is also the case for control valves and PRV.

This is especially important for all gas flow where the flow undergoes a significant pressure drop and acceleration. Conservation of the stagnation enthalpy for a flowing ideal gas, for example, leads to the following approximation of

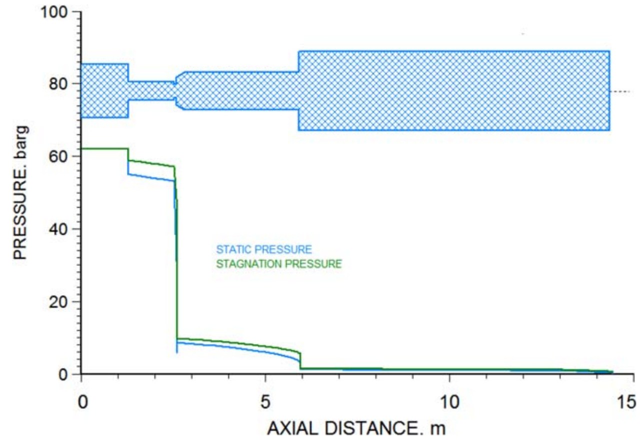

Figure 9. Case study C—Pipe segments axial pressure profiles. [Color figure can be viewed in the online issue, which is available at **wileyonlinelibrary.com**.]

temperature across the flow plane where the pressure drop is exhibited:

$$T_0 - T = \frac{1}{2}\frac{u^2}{C_p} \tag{4}$$

where T_0 is the stagnation absolute temperature. The above equation indicates that for methane flow, for example, a single velocity head loss at choked flow conditions (350 m/s) will yield a fluid temperature drop of 29.2°C, assuming an average heat capacity of 2,100 J/kg/°C. The presence of multiple pipe expansions downstream of the flow limiting orifice of a depressuring, control, or relief valve exacerbates the cold temperature potential.

We consider the steady-state flow of a high pressure gas mixture that is rich in methane through a depressuring relief line with multiple expansions, as illustrated in Figure 9. The estimates were calculated using SuperChems Expert^{TM}. We note that the starting pressure is high enough to cause multiple chokes in the downstream piping (not a recommended practice due to increased pipe failure potential from vibration risk). The steady-state pipe flow estimates in SuperChems Expert^{TM} integrate the conservation equations along the pipe axis using real fluid behavior and consider heat transfer across the pipe wall. In this particular case study, heat transfer across the pipe wall to the surroundings is considered negligible.

The calculated fluid velocity profile is illustrated in Figure 10. Multiple chokes were reached at the piping expansion locations. The speed of sound is calculated separately based on temperature, pressure, and composition by SuperChems Expert^{TM} as an independent check on the quality of the flow estimate.

The calculated temperature profiles are illustrated in Figure 11. We observe significant temperature drop and recovery associated with the pipe change in area. The flow approaches the dew point at the depressuring valve (first choke point) and also at the second choke point. If we were to consider that the pipe wall temperature is at the fluid temperature, this depressuring line would have to be constructed out of stainless steel.

For high speed, noncondensing gas/vapor flow, it is expected that the flow velocity at the inner surface of the pipe would reach zero. As a result, a large fraction of the kinetic energy is recovered as temperature at the pipe inner

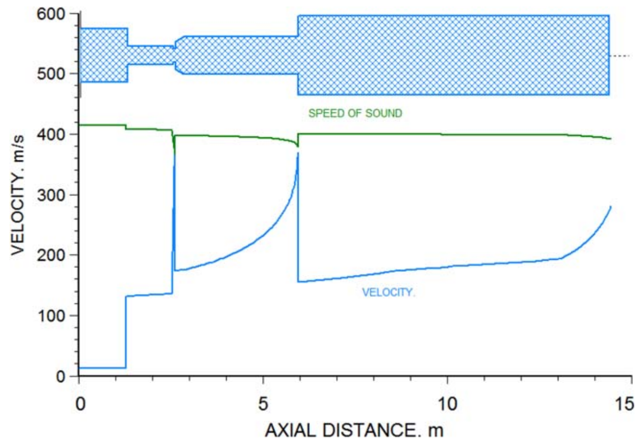

Figure 10. Case study C—Pipe segments velocity profiles. [Color figure can be viewed in the online issue, which is available at **wileyonlinelibrary.com**.]

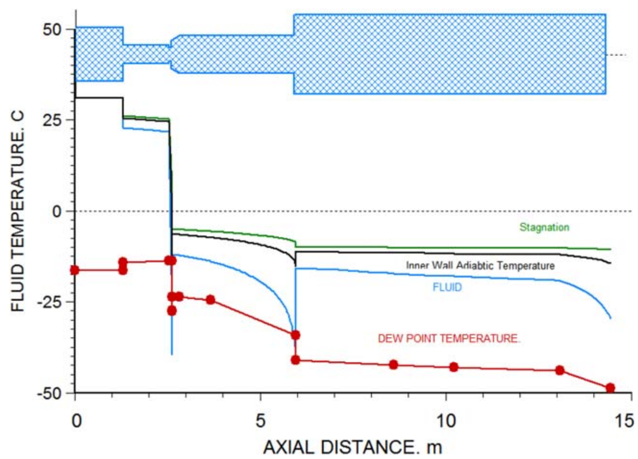

Figure 11. Case study C—Piping segments temperature profiles. [Color figure can be viewed in the online issue, which is available at **wileyonlinelibrary.com**.]

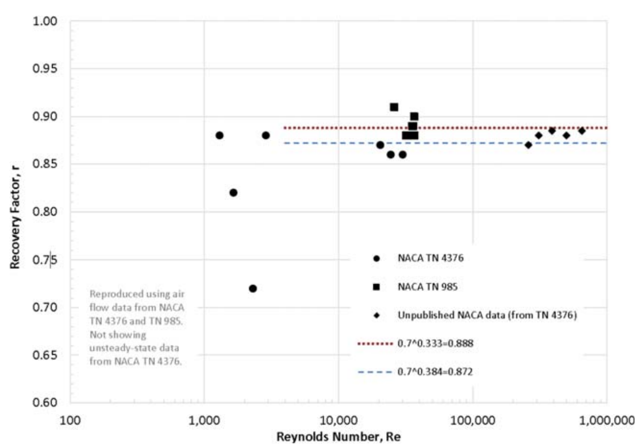

Figure 12. Measured values for the wall temperature recovery factor [8]. [Color figure can be viewed in the online issue, which is available at **wileyonlinelibrary.com**.]

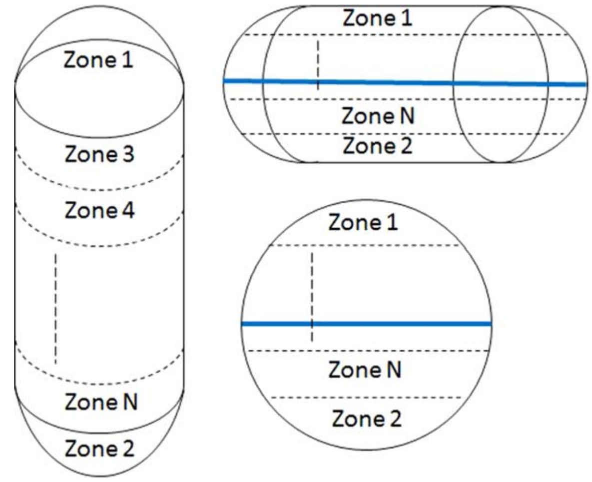

Figure 13. SuperChems expert vessel segmentation scheme. [Color figure can be viewed in the online issue, which is available at **wileyonlinelibrary.com**.]

wall surface. This is shown in Figure 11 as the inner wall adiabatic temperature and is significantly higher than the fluid temperature. This temperature recovery is typically not considered in relief systems estimates, and only becomes important for high speed noncondensing gas flow, typically at Mach numbers in excess of 1/2.

Shackelford [8] pointed out in a recent publication that the recovery factor has been experimentally measured and is approximately 0.87 for turbulent flow:

$$r = \frac{T_w - T}{T_0 - T} \approx 0.87 \tag{5}$$

where r is the recovery factor, T_w is the adiabatic inner pipe wall temperature, T is the flowing gas temperature, and T_0 is the stagnation temperature. This is also illustrated in Figure 12.

BRIEF OVERVIEW OF THE SUPERCHEMS EXPERT^{TM} FLOW DYNAMICS MODELS

The case studies considered in this article were modeled using the commercial software package SuperChems Expert^{TM}, a component of the ioMosaic Process Safety Office^{TM} suite. SuperChems Expert^{TM} solves the time-dependent detailed material, momentum, phase behavior, and energy balances for single and/or multiple interconnected vessels with complex piping for single and multiphase flow. Vapor/liquid disengagement dynamics, as well as reaction systems, are seamlessly handled for vessel and piping flow. The AIChE Design Institute for Emergency Relief Systems (DiERS) markets and sells SuperChems^{TM} for DiERS (a subset of SuperChems Expert) that is capable of simulating all the case studies considered in this article.

A unique aspect of the SuperChems^{TM} computer code is how the vessels are segmented and connected (see Figure 13). There is no limit on the number of segments a user can specify. The ability to define multiple segments allows the modeling of flame jet impingement. A wide variety of vessel shapes and heads, including composite vessels, connectivity options, and relief and mitigation options, are easily represented.

CONCLUSIONS

It is now possible to get a more realistic and detailed estimate of vessel and piping components failure potential using the SuperChems^{TM} modeling dynamics and the new fire flux equation presented in API-521 [1].

The simple heating rate equations published by API-521 and NFPA-30 should not be used to assess vessel integrity. It is also recommended that these equations should also be multiplied by a FF when used for relief sizing, especially for fuels like LNG.

The poor natural convection heat transfer characteristics of vapor/gas in gas filled vessel prevents the vessel walls from reaching cryogenic temperatures during rapid depressuring for high pressure systems and noncondensing flows.

Pipe wall temperatures for noncondensing high speed gas flows, can be substantially higher than the flowing gas temperatures, especially for Mach numbers in excess of 0.5.

LITERATURE CITED

1. API, API Standard 521 – Pressure Relieving and Depressuring Systems, Sixth Edition, 2013.
2. NFPA, NFPA-30 Flammable and Combustible Liquids Code, 2008 Edition.
3. G.A. Melhem, Advanced Consequence Analysis; Fluid Flow, Emergency Relief Systems Design, Thermal Hazards Assessment, Emission, Dispersion, Fire and Explosion Dynamics, ioMosaic Corporation, 2006.
4. E. Zamejc, API Standard 521 new alternative method to evaluate fire relief for pressure relief device sizing and depressuring system design, J Loss Prev Process Ind 27 (2014), 21–31.
5. G.A. Melhem, “Proper calculations of pipe and vessel wall temperatures during relief and/or depressurization,” API-521 Committee, 78th Fall Refining and Equipment Standards Meeting, New Orleans, November 2013.
6. B. Droste and W. Schoen, Full scale tests with unprotected and thermal insulated LPG storage tanks, J Hazard Mater 20 (1988), 41–53.
7. M.A. Haque, S.M. Richardson, and G. Saville, Blowdown of pressure vessels – I. Computer model, Trans IChemE 70 (1992).
8. A. Shackelford, Adiabatic Wall Temperature High Velocity Compressible Gas Flow, Inglenook Engineering, 2013.